

A Novel Approach to Microcalcification Detection Using Fuzzy Logic Technique

Heng-Da Cheng,* *Senior Member, IEEE*, Yui Man Lui, and Rita I. Freimanis

Abstract—Breast cancer continues to be a significant public health problem in the United States. Approximately, 182 000 new cases of breast cancer are diagnosed and 46 000 women die of breast cancer each year. Even more disturbing is the fact that one out of eight women in the United States will develop breast cancer at some point during her lifetime. Since the cause of breast cancer remains unknown, primary prevention becomes impossible. Computer-aided mammography is an important and challenging task in automated diagnosis. It has great potential over traditional interpretation of film-screen mammography in terms of efficiency and accuracy. Microcalcifications are the earliest sign of breast carcinomas and their detection is one of the key issues for breast cancer control. In this study, a novel approach to microcalcification detection based on fuzzy logic technique is presented. Microcalcifications are first enhanced based on their brightness and nonuniformity. Then, the irrelevant breast structures are excluded by a curve detector. Finally, microcalcifications are located using an iterative threshold selection method. The shapes of microcalcifications are reconstructed and the isolated pixels are removed by employing the mathematical morphology technique. The essential idea of the proposed approach is to apply a fuzzified image of a mammogram to locate the suspicious regions and to interact the fuzzified image with the original image to preserve fidelity. The major advantage of the proposed method is its ability to detect microcalcifications even in very dense breast mammograms. A series of clinical mammograms are employed to test the proposed algorithm and the performance is evaluated by the free-response receiver operating characteristic curve. The experiments aptly show that the microcalcifications can be accurately detected even in very dense mammograms using the proposed approach.

Index Terms—Breast cancer, fuzzy entropy, fuzzy logic, microcalcification, segmentation.

I. INTRODUCTION

BREAST cancer continues to be a significant public health problem in the United States. It is estimated that 182 000 new cases of breast cancer would be diagnosed and 46 000 women would die of breast cancer each year. One out of eight women will develop breast cancer at some point during her lifetime in this country. Even more disturbing is the fact that one out of eight women in the United States will develop

breast cancer at some point during her lifetime [1]. Primary prevention seems impossible since the causes of this disease still remain unknown. Early detection is the key to improving breast cancer prognosis. Mammography has been shown to be one of the most reliable methods for early detection of breast carcinomas. However, it is difficult for radiologists to provide accurate and uniform interpretation for the enormous amount of mammograms generated in widespread screening. Recently, computer-aided mammographic screening [2], [3] has received great attention because of its speed and consistency and could provide a promising solution to this task.

An early sign of disease in 30%–50% of mammographically detected cases is the appearance of clusters of fine, granular microcalcifications [4]–[10]. Sometimes, microcalcifications are the only mammographic sign in early breast cancer [9], [11], [12]. Detecting microcalcifications at an early stage is necessary so that the proper treatment can be effectively applied. Automated detection of microcalcifications can be an efficient tool for mammographic screening process.

Although computer-aided mammography has been studied over the last two decades, automated interpretation of microcalcifications still remains very difficult. The major reasons are as follows. First, the objects of interest can be extremely small, leading to potential misidentification. Second, different sizes, various shapes, and variable distributions of microcalcifications appear in mammograms, therefore, sample matching seems to be impossible. Third, the regions of interest (ROI's) may be of low contrast. The intensity difference between suspicious areas and their surrounding tissues can be quite slim. Fourth, the dense tissues and/or skin thickening, especially in younger women, cause suspicious areas to be almost invisible. Finally, dense tissues may be easily misinterpreted as calcifications yielding a high false-positive (FP) rate that is a major problem with most of the algorithms.

To deal with these problems, many methods for automated digital mammography processing have been studied. Spiesberger [13] described a computer-aided mammographic screening algorithm. Brightness, compactness, and statistics measures are applied in a decision tree to characterize the candidates. Cross-correlation coefficient is then used to measure the presence of microcalcifications. If the cross-correlation coefficient is larger than a threshold which is set to 0.65, then microcalcifications are declared. Davies *et al.* [14]–[16] used a local thresholding technique to segment clustered microcalcifications. The local threshold is selected from the valley when the local histogram is bimodal. If the local histogram is unimodal, then the subimage is interpolated from

Manuscript received September 12, 1996; revised April 23, 1998. The Associate Editor responsible for coordinating the review of this paper and recommending its publication was A. E. Burgess. Asterisk indicates corresponding author.

*H.-D. Cheng is with the Department of Computer Science, Utah State University, Logan, UT 84322 USA (e-mail: cheng@hengda.ce.usu.edu).

Y. M. Lui is with the Department of Computer Science, Utah State University, Logan, UT 84322 USA

R. I. Freimanis is with the Department of Radiology, The Bowman Gray School of Medicine, Winston-Salem, NC 27157 USA.

Publisher Item Identifier S 0278-0062(98)06446-5.

its neighbor subimages. The segmented objects are analyzed using size, shape, and gradient measures to extract clusters of microcalcifications. This method segments microcalcifications only based on the intensities of an image. It may not be correct and would affect the further processes. Shen *et al.* [17] discussed different shape factors including compactness, moments, and Fourier descriptors in calcification analysis. These quantitative measures represent the roughness of shapes and are used to classify calcifications in mammograms. They conclude that the combination of these three measures is better than just using only one or two. Fam *et al.* [18] proposed a method for the detection of fine-clustered calcifications. In their studies, if a pixel intensity falls in a specific range, the region-growing algorithm is applied and the intensity gradient is computed to test whether the candidate pixel satisfies the mean and variance criteria. The problem of this algorithm is that it requires many user-input variables. These variables are actually image dependent and should be determined automatically. Chan *et al.* [4], [5] described an algorithm for microcalcification segmentation. The difference between the enhanced image and suppressed image is calculated. A local thresholding technique is then used to segment the image. Finally, clustered microcalcifications are identified by a criterion in which a preselected number of pixels within a region is used. Monte Carlo simulated microcalcifications are employed to test this algorithm, but no results of clinical mammograms have been reported. Mascio *et al.* [19] introduced a method for microcalcification segmentation in high-resolution digital mammograms. The enhanced image is obtained by the round high-emphasis technique which is a high-pass filter preserving round edges and texture gist which is the average of morphological opening and closing subtracted from the original image. A threshold technique is then applied to segment the microcalcifications. This method is limited to detect round shape microcalcifications. However, microcalcifications often occur as variable shapes. Dengler *et al.* [20] introduced an algorithm of microcalcification segmentation. First, a high-pass filtering is performed by subtracting the low-pass Gaussian filtered image from the original image. Then, the difference between a detected spot and its neighbor spots is computed by the Gaussian operation with different weights. If the difference is less than a threshold, this spot is not considered to be a microcalcification. The threshold is determined to be $2.5 \times$ the global standard derivation that is derived from the image after the Gaussian operation. The segmented image is used as a mask and the intensities of the pixels below this threshold are used to recalculate the standard deviation. The final threshold is chosen as $3 \times$ the standard derivation. Finally, eight structure elements are employed to reconstruct the shapes of microcalcifications. Chan *et al.* [37] stated that the detection accuracy by computer decreased as the pixel size increased from $0.035 \text{ mm} \times 0.035 \text{ mm}$, and evaluated two compression methods and the effects on computerized detection of subtle microcalcifications. They concluded that the discrete cosine transform with full frame entropy coding (DCT-FFEC) method with bit splitting is more efficient than the Laplacian pyramid hierarchical coding (LPHC) method with linear quantization for compression of

mammographic images, without degradation of the detectability of subtle microcalcifications. The highest compression rate without significant loss in detection accuracy was 9.6 : 1.

In this paper, we attempt to overcome the problems introduced by the existing algorithms, and propose a novel approach to detecting the microcalcification clusters in arbitrary shape and in the mammograms of the breasts with various densities, and to reduce computational burden. The proposed algorithm consists of the following five major steps: image fuzzification, image enhancement, irrelevant breast-structure removal, segmentation, and image reconstruction. Global information (brightness) and local information (nonuniformity) are exerted to produce a fuzzified image and an enhanced image. Moreover, the irrelevant breast-structures are eliminated by the proposed curve detector. An iterative threshold is then used to locate the microcalcifications. Finally, the microcalcifications are reconstructed by mathematical morphology techniques. A series of clinical mammograms are employed to test the proposed algorithm. The experiments aptly show that the microcalcifications can be accurately located even for very dense mammograms, but most of their features are also well preserved.

The organization of the rest of this paper is as follows. The data acquisition is illustrated in Section II. The proposed method is presented in Section III. The experimental results and conclusions are given in Sections IV and V, respectively.

II. DATA ACQUISITION

The mammographic images were obtained by direct digital acquisition using a Phillips Computed Radiography System in the Department of Radiology, Bowman Gray School of Medicine/North Carolina Baptist Hospital. Images were obtained from sequential patients who presented for needle localization prior to surgical biopsy for mammographic nonpalpable abnormalities. Normally, we obtain preliminary lateral-medial, and craniocaudal views of the breast to be biopsied, just prior to needle localization, to verify location of the abnormality for accurate targeting. Therefore, no additional radiation was received by the patients in obtaining these images. In this study, a total of 75 mammographic images were selected. All of them had been read by radiologist with mammographic expertise and proven by biopsies. Among them, 60 are abnormal and 15 normal. The size of the images is 2510×2000 pixels with 1024 gray levels. The pixel size is $0.1 \text{ mm} \times 0.1 \text{ mm}$. Before applying the proposed approach, ROI's of images were located by a radiologist with specialization in mammography. The calcifications presented as clusters containing two or more detected pixels within a 15×15 box. The formats of ROI are fixed to 256×256 pixels with 256 gray levels due to the limit of the hardware available.

III. PROPOSED APPROACH

The aim of this study is to develop an algorithm to detect microcalcifications in mammograms of the breasts with various densities. The digital mammographic images are the only inputs of the proposed algorithm and no other information is required. The proposed method consists of five major steps:

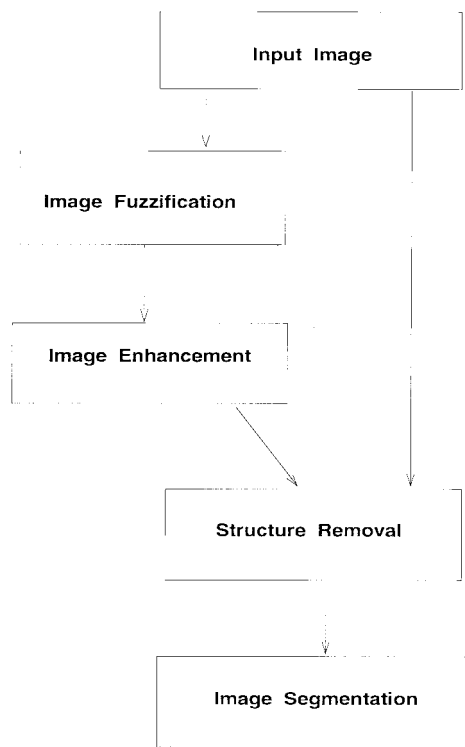


Fig. 1. The system diagram of the proposed algorithm.

image fuzzification, image enhancement, irrelevant breast-structure removal, segmentation, and image reconstruction. A schematic diagram of the proposed approach is given in Fig. 1.

In step 1, global information (intensity) is employed to transform an image to a fuzzified image using a π function. The cross-over point, which corresponds to the intensity of microcalcifications, is determined automatically. Local information (geometrical statistics) is then employed to compute the nonuniformity in step 2, and will interact with the fuzzified information. These two factors are used as microcalcification enhancement criteria. Due to a wide variety of breast tissues, some unwanted breast structures may be enhanced with microcalcifications. These breast structures are removed in step 3. We found that most of these breast structures are curve-like patterns after the microcalcification enhancement. A modified curve detector is applied to remove these irrelevant details but to preserve the shapes of microcalcifications. This procedure takes the enhanced image as an input and interacts the enhanced image with the original image to preserve the shapes of microcalcifications. After irrelevant breast-structure removal, an iterative threshold selection method is applied to locate the microcalcifications in step 4. A morphological operator, close-opening, is adopted to reconstruct the shapes of microcalcifications in step 5. Finally, microcalcifications are located. The main advantage of this paper is that by using a fuzzified image and the proper thresholding technique as well as the modified curve detector, the microcalcifications can be effectively detected even in very dense mammograms.

A. Microcalcification Enhancement

Since many mammograms do not have sufficient contrast to allow easy detection of microcalcifications, mammographic

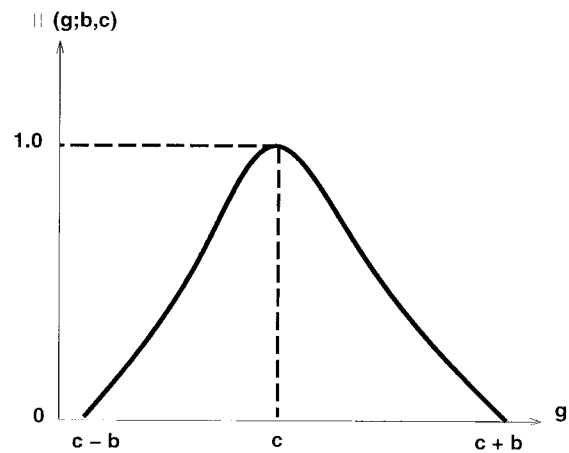


Fig. 2. A π function.

enhancement is still an essential and first step of digital mammographic processing. A common assumption in digital mammography is that the suspicious areas are brighter than their surrounding tissues [21]. Dhawan *et al.* [22] described a contrast histogram whose low region might belong to the fat tissues and the high region might belong to features. Similarly, the basic postulate of the proposed method is that the intensities of microcalcifications are higher than the average intensity of the breast tissues. In addition, the regions of microcalcifications are usually inhomogeneous. The proposed enhancement technique employs fuzzy set theory and geometrical statistics to increase the contrast of microcalcifications. First, the original image is transformed to a fuzzified image according to the brightness, then, the nonuniformity of the regions is measured using geometrical statistics.

Fuzzy set theory has been proven to be useful in many areas of image processing [23]–[25]. It is well known that mammographic images have some degrees of fuzziness such as indistinct borders, ill-defined shapes, and different densities. *Due to the nature of mammography and breast structure, fuzzy logic would be a better choice to handle the fuzziness of mammograms than traditional methods.* In this study, fuzzy logic is employed to accomplish this objective. First, the intensities of an image are transformed to an interval $[0, 1]$ using a π function [26] shown in Fig. 2. The values of the π function represent the degrees of the closeness of being microcalcifications in terms of intensities. The π function is, therefore, used to locate the intensities of microcalcifications. The selection of a cross-over point could be viewed as an object-background classification problem, and the thresholding techniques [27], [28] can be applied. Valley-seeking approaches are usually utilized to select a threshold if the histogram is bimodal. However, histograms would not always be bimodal, especially in medical images. The fuzzy region of the π function is chosen as the range from the mean intensity to the maximum intensity of the image, since the proposed approach assumes that the intensities of microcalcifications are higher than the average intensity of breast tissues. It implies that the intensities of microcalcifications are located somewhere between the mean intensity and the maximum intensity of an image. The intensities of microcalcifications correspond to the cross-

over point. The cross-over point selection using the entropy thresholding method [29] is briefly described as the following.

Let p_1, p_{k+1}, \dots, p_N be the probability distribution of grey levels. The object and background distributions are shown as follows:

Picture Background:

$$\frac{p_1}{P_{k-1}}, \frac{p_2}{P_{k-1}}, \dots, \frac{p_{k-1}}{P_{k-1}}. \quad (1)$$

Tissue Background:

$$\frac{p_k}{P_t - P_{k-1}}, \frac{p_{k+1}}{P_t - P_{k-1}}, \dots, \frac{p_t}{P_t - P_{k-1}}. \quad (2)$$

Object:

$$\frac{p_{t+1}}{1 - P_t}, \frac{p_{t+2}}{1 - P_t}, \dots, \frac{p_N}{1 - P_t}. \quad (3)$$

where $P_{k-1} = \sum_{i=1}^{k-1} p_i$, $P_t = \sum_{j=1}^t p_j$, t is the value of the threshold, k is the value of the mean intensity, and N is the maximum intensity of the image.

Since we want to separate microcalcifications from the tissue background, the picture background is not interested and can be ignored in this study. Mammographic images would, however, contain tremendous amount of dark pixels. It could affect the average intensity of the breast tissues. Hence, the mean value of the breast tissues is defined as follows by excluding these dark pixels

$$k = \frac{1}{W} \sum_x^X \sum_{y \in G}^Y g_{xy} \quad (4)$$

where X and Y are the dimensions of the image, G is the region having intensities larger than 100, W is the number of pixels in this region and g_{xy} is the grey level at the coordinates x and y .

An alternative approach to calculate the approximate mean of an image is to find the grey level corresponding to the peak of the histogram which represents the maximum number of occurrences. The experiments show that these two mean values are quite close, and both can provide good measurements of breast tissues.

Then, the entropies of the object and background distributions can be defined as

$$H_b(t) = - \sum_{i=k}^t \frac{p_i}{P_t - P_{k-1}} \log_e \frac{p_i}{P_t - P_{k-1}} \quad (5)$$

$$H_o(t) = - \sum_{i=t+1}^N \frac{p_i}{1 - P_t} \log_e \frac{p_i}{1 - P_t} \quad (6)$$

where $H_b(t)$ stands for the entropy of background pixels and $H_o(t)$ for the entropy of object pixels.

The maximum information of the background and object distributions can be obtained by

$$t^* = \underset{t=k}{\text{Arg max}} \{H_b(t) + H_o(t)\} \quad (7)$$

where t^* is the optimal threshold.

The value of t^* is employed as the cross-over point of the π function. The π function [26] can be computed as follows:

$$S(g; x, y, z) = \begin{cases} 0, & g \leq x \\ 2[(g-x)/(z-x)]^2, & x \leq g \leq y \\ 1 - 2[(g-z)/(z-x)]^2, & y \leq g \leq z \\ 1, & g \geq z \end{cases} \quad (8)$$

$$\pi(g; b, c) = \begin{cases} S(g; c-b, c-b/2, c), & \text{if } g \leq c \\ 1 - S(g; c, c+b/2, c+b), & \text{otherwise} \end{cases} \quad (9)$$

where g is the intensity, c is the cross-over point and let $c = t^*$, and b is the fuzzy bandwidth defined as:

$$b = \max\{(c-k), (N-c)\} \quad (10)$$

where k is the mean value, and N is the maximum intensity of the image.

We use π function to fuzzify the original image. The fuzzy π function (9) is constructed to locate the intensities of microcalcifications. Based on information theory, it maximizes the information between tissue background and microcalcifications. The merit of using fuzzy set is its ability to handle uncertainty and its robustness.

After considering the intensity brightness, the local information is also used as the enhancement criterion. Local geometrical information is employed to measure the nonuniformity of the image. First, local variances are computed

$$\mu_{xy} = \frac{1}{M \times M} \sum_{j=1}^M g_j \quad (11)$$

$$[\sigma_{xy}^2] = \left[\frac{1}{M \times M} \sum_{j=1}^M (g_j - \mu_{xy})^2 \right] \quad (12)$$

where μ_{xy} is the local mean, σ_{xy}^2 is the local variance, x and y are the coordinates of the current pixel, and M is the dimension of the window, and g_j is the intensity. In our experiments, M is equal to five, which is related to the maximum size of microcalcifications.

The local variance occurrence function (i.e., the histogram of local variances) is then calculated

$$h(q) = \sum_{q=0}^V \delta([\sigma_{xy}^2] - q) \quad (13)$$

$$\delta(t) = \begin{cases} 1, & t = 0 \\ 0, & \text{otherwise} \end{cases} \quad (14)$$

where x and y are the coordinates of the locations where the variances were computed, $1 \leq x, y \leq M$, and g is the gray level, $g = 0, 1, \dots, V$. Experiments show that the local variance occurrence function contains nothing significance when V is greater than 100.

The areas containing microcalcifications (i.e., ROI) are usually inhomogeneous and the variances of these areas would be larger than those of tissue background regions. Therefore, a threshold can be used to separate the microcalcifications from the breast tissues according to nonuniformity. This threshold is found from the local variance occurrence function (13) and determined by the minimum error thresholding technique [30].

The minimum error thresholding technique is derived under a normal distribution. Ye *et al.* [31] suggested two ways to implement this technique. One is to minimize the criterion function and the other is to search a threshold iteratively. In our experiments, we employ the minimization criterion function [30] briefly explained as follows.

If we consider a normal distribution with mean μ_i , standard deviation σ_i , and a *a priori* probability P_i , then the probability density function $p(g)$ could be written as

$$p(g) = \sum_{i=1}^C P_i p(g|i) \quad (15)$$

$$p(g|i) = \frac{1}{\sqrt{2\pi}\sigma_i} \exp\left(-\frac{(g-\mu_i)^2}{2\sigma_i^2}\right) \quad (16)$$

where g is a grey level, C is the number of classes, and $p(g|i)$ is the conditional probability density function. Our objective is to classify microcalcifications and tissue background, therefore, C is equal to two.

By considering a two class problem ($C1$ background and $C2$ object), a fitting technique can be applied to estimate the parameters from the histogram as follows:

$$P_1(T) = \sum_{g=0}^T h(g) \quad (17)$$

$$P_2(T) = \sum_{g=T+1}^N h(g) \quad (18)$$

$$\mu_1(T) = \left[\sum_{g=0}^T h(g)g \right] / P_1(T) \quad (19)$$

$$\mu_2(T) = \left[\sum_{g=T+1}^N h(g)g \right] / P_2(T) \quad (20)$$

$$\sigma_1(T) = \left[\sum_{g=0}^T (g - \mu_1(T))^2 h(g) \right] / P_1(T) \quad (21)$$

$$\sigma_2(T) = \left[\sum_{g=T+1}^N (g - \mu_2(T))^2 h(g) \right] / P_2(T) \quad (22)$$

where T is an arbitrary gray level, $h(g)$ is the probability of a gray level g , N is the maximum intensity, P is the probability of the class, μ is the mean, and σ is the variance of the class.

Using the Bayes classifier, the classification error for two classes would be

$$\varepsilon(g, T) = \left[\frac{(g - \mu_i(T))}{\sigma_i} \right]^2 + 2 \log_e \sigma_i(T) - 2 \log_e P_i(T) \quad (23)$$

where

$$i = \begin{cases} 1, & g \leq T \\ 2, & g > T. \end{cases} \quad (24)$$

Then, the minimum-error thresholding criterion would be

$$J(T) = \min_T \sum_g h(g) \cdot \varepsilon(g, T) \quad (25)$$

where T is the optimum threshold.

Substituting the parameters [from (17) to (23)] into the criterion $J(T)$ (25), we can find

$$J(T) = 1 + 2[P_1(T) \log_e \sigma_1(T) + P_2(T) \log_e \sigma_2(T)] - 2[P_1(T) \log_e P_1(T) + P_2(T) \log_e P_2(T)]. \quad (26)$$

By employing a fitting technique, the optimum threshold T is found corresponding to the minimum value of $J(T)$. Then, the nonuniformity factor ν_i may be computed and transformed to the interval $[0, 1]$ by classifying the local variance occurrence function (13) to be background (uniformity) and object (nonuniformity) shown as follows:

$$\nu_i = \begin{cases} \sigma_i^2/T, & \text{if } \sigma_i^2 \leq T \\ 1, & \text{otherwise} \end{cases} \quad (27)$$

where T is the optimum threshold determined in (25), σ_i^2 is the local variance, and i is the pixel index.

Combining (9) and (27), a new enhanced image is obtained:

$$g' = \pi(g; b, c) \times \nu_i \times N \quad (28)$$

where N is the maximum intensity of an image.

In accordance with information theory, the maximum information about microcalcifications and tissue background is obtained through the proposed image fuzzification procedure based on the maximum fuzzy entropy principle. The nonuniformity is also considered as a factor of microcalcification enhancement. Hence, microcalcifications are enhanced and the suspicious areas are revealed by the nonuniformity of the regions and the brightness.

B. Irrelevant Breast Structure Removal

Due to the variety of breast tissues, the irrelevant structures of breasts need to be removed. Most of the irrelevant breast-structures were found to exhibit line-like or curve-like patterns after the microcalcification enhancement. A curve detector is, therefore, employed to remove these irrelevant breast structures. The proposed curve-detection algorithm is a modified version of the one in [32].

The following definitions are needed to facilitate our discussion about the proposed curve detector. Let d_1, d_2, \dots , and d_8 be the absolute intensity differences between the current pixel and its eight neighbors shown in Fig. 3. The proposed curve detector will trace four different directions, namely, UP, DOWN, LEFT, and RIGHT. D_{UP} , D_{DN} , D_L , and D_R represent the number of pixels followed along the corresponding directions. The current pixel is considered to be connected to its neighbors if at least one of the following conditions is encountered:

$$\begin{aligned} \text{UP:} & \quad \min(d_2, d_3, d_4) < T \\ \text{DOWN:} & \quad \min(d_6, d_7, d_8) < T \\ \text{LEFT:} & \quad \min(d_4, d_5, d_6) < T \\ \text{RIGHT:} & \quad \min(d_1, d_2, d_8) < T \end{aligned}$$

where T is the maximum allowed difference between a current pixel and its connected neighbor pixels. In our study, T is set to five.

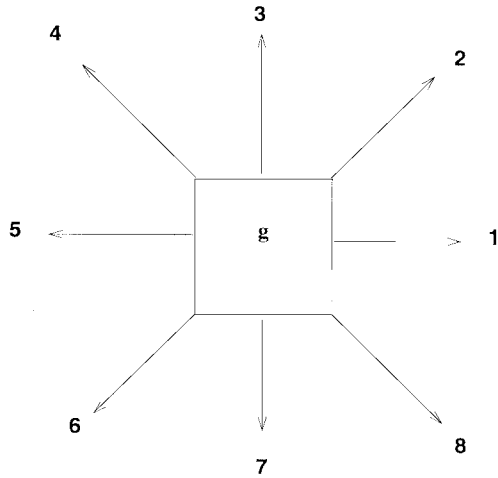


Fig. 3. The direction indexes of each pixel.

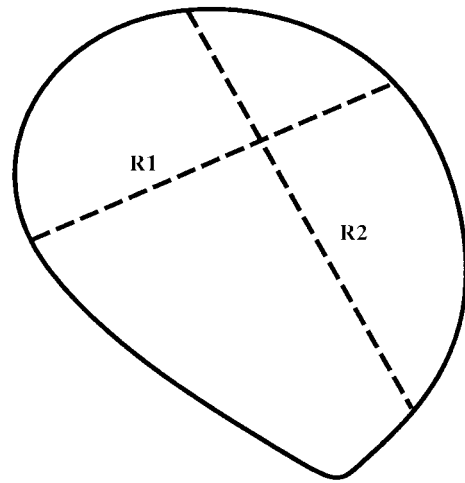


Fig. 4. Example of a microcalcification.

The neighbor pixel is connected with the current pixel if the absolute value of the grey level difference is minimum. Otherwise, the curve tracing is terminated on that direction. In addition, the initial order of curve tracing is predefined to ensure that the length and width are followed correctly. The indexes UP (2, 3, and 4), DOWN (6, 7, and 8), LEFT (4, 5, and 6), and RIGHT (2, 1, and 8) are denoted as d_{up} , d_{dn} , d_l , and d_r , respectively. Only the enhanced pixels are considered and all of the pixels are the initial pixels (Here, we can see the parallel nature of the proposed approach which is not discussed in this paper.) The rules for initial tracing direction settings are given as follows:

if $\{(d_{up} = 3 \text{ and } d_{dn} = 7) \text{ or } (d_{up} = 2 \text{ and } d_{dn} = 8),$
 or $(d_{up} = 4 \text{ and } d_{dn} = 6)\}$
 $\{d_l = 5; d_r = 1;\},$
 else $\{$ if $(d_{up} = 2)$, then $d_r = 8;$
 if $(d_{up} = 3)$, then $d_r = 1;$
 if $(d_{up} = 4)$, then $d_r = 2;$
 if $(d_{dn} = 6)$, then $d_l = 4;$
 if $(d_{dn} = 7)$, then $d_l = 5;$
 if $(d_{dn} = 8)$, then $d_l = 6\}$

when UP or DOWN does not have any connected neighbor, the default directions of d_r and d_l are set to one and five, respectively.

The goal of the proposed curve detector is to remove the irrelevant curve-like breast structures but preserve the shapes of microcalcifications such that high fidelity can be achieved. Generally, whether a pixel is considered as a microcalcification or a curve-like pattern it can be determined by the ratio of its tracing length and width. If the tracing length and width are similar, then a microcalcification is found (see Fig. 4), otherwise, a curve-like pattern is declared (see Fig. 5) and should be deleted. Formally, a current pixel is declared to be

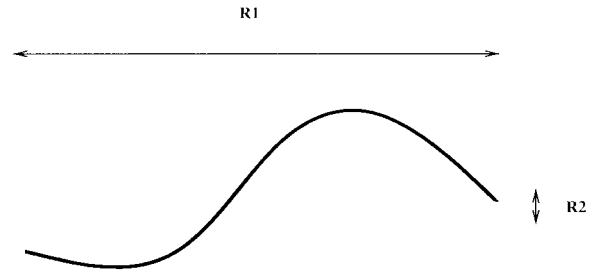


Fig. 5. The direction indexes of each pixel.

on a curve if it satisfies one of the following two conditions:

$$R_1 = D_{UP} + D_{DN}$$

$$R_2 = D_L + D_R$$

$$R = \frac{\max(R_1, R_2)}{\min(R_1, R_2)}$$

Condition 1: $R > T_1$

Condition 2: $\max(R_1, R_2) > T_2.$

Condition 1 states that a curve is found if the ratio of the length and the width is greater than T_1 . And, condition 2 demonstrates that a curve is detected if the length or width is greater than T_2 . In our study, we found that the breast-structure detector would be optimal if T_1 was set to four and T_2 is set to 20 through the experiments.

Thereafter, the irrelevant breast structures are removed by the proposed curve detector. The proposed curve detector interacts with both the enhanced image and the original image, in other words, two images are utilized by the proposed curve detector. First, a pixel of an enhanced image is viewed as a candidate pixel. The curve detector would trace its length and width from the original image to determine whether a pixel should be preserved or removed. The advantages of interacting with the enhanced image and the original image exhibit the reduction of search space and the use of high fidelity of the original data.

C. Microcalcification Segmentation and Reconstruction

Microcalcification segmentation is performed based on the result of image enhancement and irrelevant breast-structure removal. An iterative threshold selection method [33] is employed to implement the segmentation process. This technique selects the threshold iteratively. First, the input image is averaged to find an initial threshold, T_0 . This threshold is then used to segment the image, and the newly segmented image is represented as a new input image. The same procedure can then be repeated until the maximum number of iterations is reached, or the change of threshold values ($\text{abs}(T_i - T_{i-1})$) is less than ϵ , a preset value. In our experiments, the maximum number of iterations is equal to ten and ϵ is set to three. In order to speed up the process, the pixels whose grey levels are less than 100 are not used to compute the average value.

Mathematical morphology is a powerful tool for image shape analysis [34]. Binary morphological operators are employed to reconstruct the shapes of the microcalcifications and to remove isolated pixels. The basic binary morphological operators, reflection, dilation, and erosion, are defined as follows:

Reflection:

$$\hat{B} = \{x | x = -b, \text{ for } b \in B\}. \quad (29)$$

Dilation:

$$A \oplus B = \{x | (\hat{B})_x \cap A \neq \emptyset\}. \quad (30)$$

Erosion:

$$A \ominus B = \{x | (B)_x \subseteq A\}. \quad (31)$$

where A is an image and B is a small image called structure element. In our experiments, a 2×2 square structure element is employed.

After defining these basic binary morphological operators, two important operators called opening and closing can be described as follows:

Opening:

$$A \circ B = (A \ominus B) \oplus B. \quad (32)$$

Closing:

$$A \bullet B = (A \oplus B) \ominus B. \quad (33)$$

Opening has an effect to smooth the contour and to eliminate thin protrusions of an image. Closing can fill small holes and gaps in the contour of an image. The microcalcification reconstruction is performed by the combined operator called close-opening

$$(A \bullet B) \circ B. \quad (34)$$

After performing morphological close-opening, the microcalcifications will be reconstructed to make the holes in microcalcifications be filled, and the isolated pixels be extinguished. However, opening operator may delete some spots which are not isolated. These spots could be very important since they may be used to determine some clusters based on

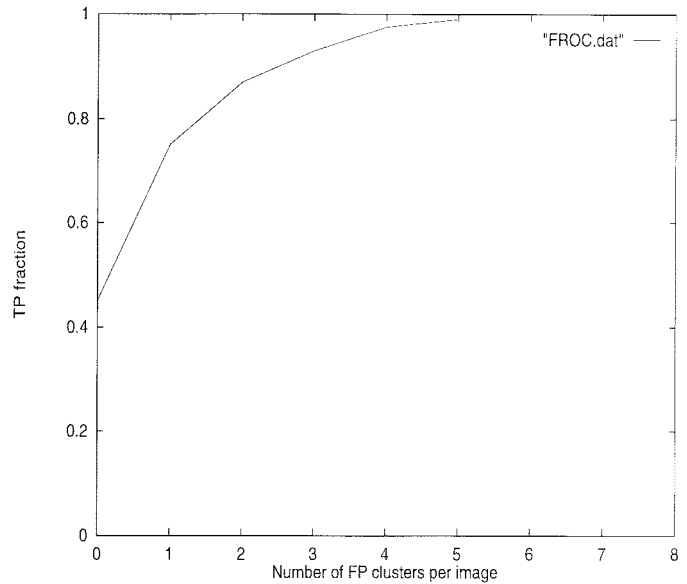


Fig. 6. FROC curve of the proposed approach.

the number of spots within a certain range. The spot-finding procedure needs to be applied. It will undelete a spot if a subregion has more than one pixel. Therefore, the grouped pixels can be recovered by comparing with the reconstructed image and the segmented image. The subregion size is set to 15×15 in our experiments. Other spots are considered to be loose clusters which are usually benign disease.

IV. EXPERIMENTAL RESULTS

In this study, 75 ROI images are employed to test the proposed algorithm. The performance of the proposed approach is evaluated by a free-response receiver operating characteristic (FROC) [35] in terms of true-positive (TP) fraction for a given number of FP clusters per image. A cluster, in our experiment, is defined as a group of microcalcification pixels (≥ 2 pixels) in an 15×15 pixel box. Moreover, a TP cluster is a detected cluster which has overlapped more than 50% with the suspicious area identified by a radiologist. All other clusters are considered to be FP clusters. The detection accuracy of the proposed algorithm is evaluated by a FROC curve shown in Fig. 6. It reveals the tradeoff between TP fraction and the number of FP clusters per image using the proposed approach. The FROC curve shows that the proposed method can archive a greater than 96% TP rate with the FP rate of four clusters per image. However, FROC analysis suffers from its limitations [36]. For instance, it does not address the complexity of images. It is also a difficult task to transform the subjective measurements (radiologist's observations) to the objective FROC curve.

The following images are used to demonstrate the robustness of the proposed approach. A dense mammogram is given in Fig. 7(a). Its enhanced image and the image after irrelevant breast-structure removal are shown in Fig. 7(b) and (c), respectively. The finally segmented result is given in Fig. 7(d). The result shows that the microcalcifications are not only located and their main features (linear distribution

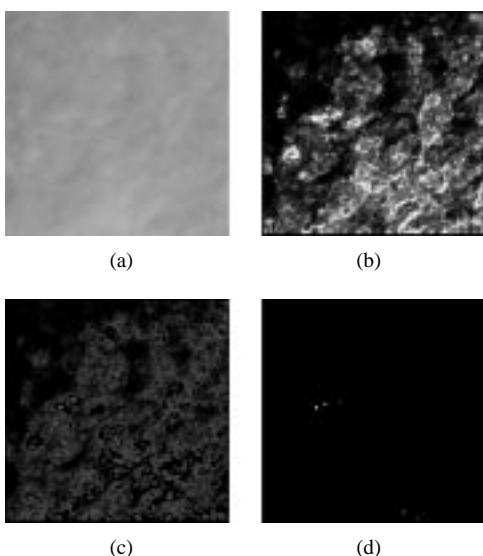


Fig. 7. (a) The original mammogram image, (b) enhanced image, (c) enhanced image after irrelevant breast-structure removal, and (d) final resulting image.

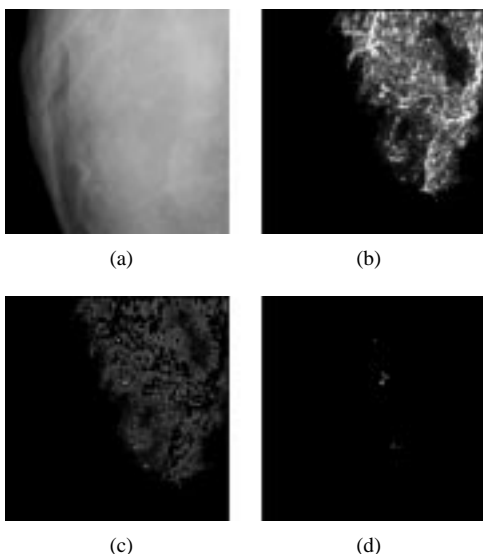


Fig. 8. (a) The original mammogram image, (b) enhanced image, (c) enhanced image after irrelevant breast-structure removal, and (d) final resulting image.

of microcalcifications) are also well preserved. It would be difficult to distinguish those microcalcifications from the original image shown in Fig. 7(a). The results facilitate the further processes such as categorizing the lesions into benign and malignant. Another test mammogram is shown in Fig. 8(a). The mammogram contains a lot of dense tissues. Its enhanced image is given in Fig. 8(b). As we can see, most of the irrelevant breast structures are also enhanced with the microcalcifications. Nevertheless, the microcalcifications emerge clearly after irrelevant breast-structure removal as shown in Fig. 8(c). This figure demonstrates that the irrelevant breast structures can be easily excluded but the microcalcifications are well preserved. The finally segmented image [refer to Fig. 8(d)] reveals that the microcalcifications are extracted successfully even in the mammogram of very dense breast.

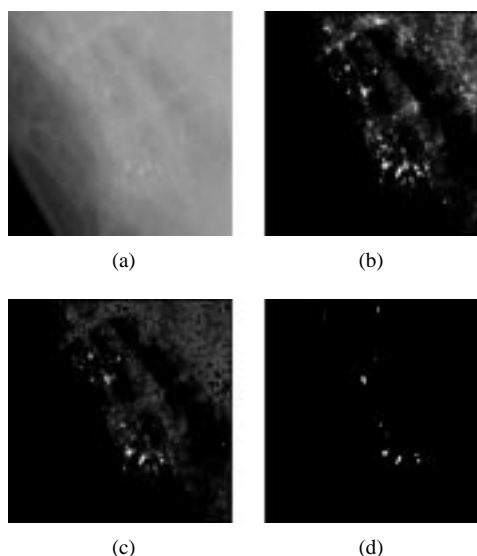


Fig. 9. (a) The original mammogram image, (b) enhanced image, (c) enhanced image after irrelevant breast-structure removal, and (d) final resulting image.

Most of the clusters in the mammogram can be detected. However, some of the clusters are almost invisible; it is extremely difficult to distinguish them even for a radiologist. An example of such mammograms is shown in Fig. 9(a). Its enhanced image, resulting image after removal of irrelevant breast-structures and the finally segmented image are shown in Fig. 9(b)–(d), respectively. Most of the clusters of the mammogram were successfully detected, however, some clusters cannot be detected that cause false negative detection as shown in Fig. 9(d). The reason for this error is that the microcalcifications are superimposed on curve-like tissues and are removed when the curve detector for removing irrelevant breast structure is applied.

In clinical applications, patients have the breasts with various densities. It is vital to detect microcalcifications in mammograms with various densities. We have considered different kinds of mammograms encountered in clinical applications and the experimental results reveal that microcalcifications are detected effectively, and the sizes, shapes and intensities of the microcalcification clusters are well preserved even in very dense breast mammograms in most of the cases. The processing time for a 256×256 ROI image consumes approximately 6 s on a SUN Ultra 1 workstation.

V. CONCLUSIONS

A novel approach using fuzzy logic to detecting microcalcifications in digitized mammograms with various densities is proposed. This approach consists of five major steps including image fuzzification, image enhancement, irrelevant breast-structure removal, segmentation, and image reconstruction. The proposed approach is very efficient for locating microcalcifications in the mammograms of the breasts with various densities, Since microcalcifications have some kinds of fuzziness, fuzzy set theory is preferable to ordinary methods for detecting microcalcifications. The key idea of the proposed method is to apply the fuzzified image to locate the ROI's and

to interact with the original image to preserve the fidelity. The advantages of the proposed approach are: 1) The microcalcifications are accurately detected even in mammograms of very dense breasts. 2) The irrelevant breast-structures can be easily identified and removed. 3) The processing time is very fast since the major computation is for global thresholding. 4) Some parameters can be adjusted in order to find out different levels of TP and FP rates. It would facilitate the computer-aided diagnosis. 5) The experimental results encourage the usage of the proposed approach for microcalcification detection and it provides a good platform for further processes such as categorizing the lesions into benign and malignant. Further improvement of the proposed approach can be achieved by using higher-resolution images [37], more powerful contrast enhancement algorithm [38], neural networks, etc.

ACKNOWLEDGMENT

The authors wish to thank the anonymous reviewers for their invaluable comments which improve the quality of the manuscript.

REFERENCES

- [1] P. A. Wingo, T. Tong, and S. Bolden, "Cancer statistics," *CA. J. Clin.*, vol. 45, pp. 8–30, 1995.
- [2] C. J. Vyborny and M. L. Giger, "Computer vision and artificial intelligence in mammography," *AJR*, vol. 162, pp. 699–708, 1994.
- [3] K. S. Woods, C. C. Doss, K. W. Bowyer, J. L. Solka, C. E. Priebe, and W. P. Kegelmeyer, Jr., "Comparative evaluation of pattern recognition techniques for detection of microcalcifications in mammography," *Int. J. Pattern Recogn. Artif. Intell.*, vol. 7, no. 6, pp. 1417–1436, 1993.
- [4] H. P. Chan, K. Doi, C. J. Vyborny, R. A. Schmidt, C. E. Metz, K. L. Lam, T. Ogura, Y. Wu, and H. MacMahon, "Improvement in radiologists' detection of clustered microcalcifications on mammograms," *Med. Phys.*, vol. 25, no. 10, pp. 1102–1110, 1990.
- [5] H. P. Chan, K. Doi, S. Galhotra, C. J. Vyborny, H. MacMahon, and P. M. Jokich, "Image feature analysis and computer-aided diagnosis in digital radiography—I. Automated detected of microcalcifications in mammography," *Med. Phys.*, vol. 14, no. 4, pp. 538–548, 1987.
- [6] H. P. Chan, K. Doi, C. J. Vyborny, R. A. Schmidt, C. E. Metz, K. L. Lam, T. Ogura, Y. Wu, and H. MacMahon, "Improvement in radiologists' detection of clustered microcalcifications on mammograms," *Med. Phys.*, vol. 25, no. 10, pp. 1102–1110, 1990.
- [7] S. L. Olson, B. W. Fam, P. F. Winter, F. J. Scholz, A. K. Lee, and S. E. Gordon, "Breast calcifications: Analysis of imaging properties," *Radiol.*, vol. 169, no. 2, pp. 329–332, 1988.
- [8] R. N. Strickland and H. I. Hahn, "Detection of microcalcifications using wavelets," in *Digital Mammography: Proceedings of the 2nd International Workshop on Digital Mammography*, A. G. Gale et al. Eds. York, U.K.: Elsevier Science, July 1994, pp. 10–12.
- [9] L. Shen, R. M. Rangayyan, and J. E. L. Desautels, "Detection and classification of mammographic calcifications," in *State of the Art in Digital Mammographic Image Analysis*, K. W. Bowyer and S. Astley, Eds. Cleveland, OH: World Scientific, 1994.
- [10] Y. Wu and K. Doi, "Computerized detection of clustered microcalcifications in digital mammograms: Applications of artificial neural networks," *Med. Phys.*, vol. 19, no. 3, May/June 1992.
- [11] L. W. Basset and R. H. Gold, *Breast Cancer Detection: Mammography and Other Methods in Breast Imaging*, 2nd ed. New York: Grune & Stratton, 1987.
- [12] E. A. Sickles, "Mammographic features of malignancy found during screening," in *Recent Results in Cancer Research*, S. Brunner and B. Langfeldt, Eds. New York: Springer-Verlag, 1990, vol. 119, pp. 88–93.
- [13] W. Spiesberger, "Mammogram inspection by computer," *IEEE Trans. Biomed. Eng.*, vol. 26, pp. 213–219, Apr. 1979.
- [14] D. H. Davies and D. R. Dance, "Automatic computer detection of clustered calcifications in digital mammograms," *Phys. Med., Biol.*, vol. 35, no. 8, pp. 1111–1118, 1990.
- [15] D. H. Davies, D. R. Dance, and C. H. Jones, "Automatic detection of clusters of calcifications," *SPIE Medical Imaging IV: Image Processing*, vol. 1233, pp. 185–191, 1990.
- [16] ———, "Automatic detection of microcalcifications in digital mammograms using local area thresholding techniques," *SPIE Medical Imaging III: Image Processing*, vol. 1092, pp. 153–157, 1989.
- [17] L. Shen, R. M. Rangayyan, and J. E. L. Desautels, "Application of shape analysis to mammographic calcification," *IEEE Trans. Med. Imag.*, vol. 13, pp. 263–274, June 1994.
- [18] B. W. Fam, S. L. Olson, P. F. Winter, and F. J. Scholz, "Algorithm for the detection of fine clustered calcifications on film mammograms," *Radiol.*, vol. 169, no. 2, pp. 333–337, 1988.
- [19] L. N. Mascio, J. M. Hernandez, and C. M. Logan, "Automated analysis for microcalcifications in high-resolution digital mammograms," *SPIE Image Processing*, vol. 1898, pp. 472–479, 1993.
- [20] J. Dengler, S. Behrens, and J. F. Desaga, "Segmentation of microcalcifications in mammograms," *IEEE Trans. Med. Imag.*, vol. 12, pp. 634–642, Dec. 1993.
- [21] H. D. Li, M. Kallergi, L. P. Clarke, V. K. Jain, and R. A. Clark, "Markov random field for tumor detection in digital mammography," *IEEE Trans. Med. Imag.*, vol. 14, pp. 565–576, Sept. 1995.
- [22] A. P. Dhawan, G. Buelloni, and R. Gordon, "Enhancement of mammographic features by optimal adaptive neighborhood image processing," *IEEE Trans. Med. Imag.*, vol. MI-5, pp. 8–15, Mar. 1986.
- [23] H. D. Cheng, C. H. Chen, and H. H. Chiu, "Fuzzy homogeneity approach to image thresholding and segmentation," *Inform. Sci.: An Int. J.*, vol. 98, nos. 1–4, pp. 237–262, 1997.
- [24] X. Li, Z. Zhao, and H. D. Cheng, "Fuzzy entropy threshold approach to breast cancer detection," *Inform. Sci., Applicat.: An Int. J.*, vol. 4, no. 1, pp. 49–56, 1995.
- [25] W. Pedrycz, "Fuzzy sets in pattern recognition: Methodology and methods," *Pattern Recogn.*, vol. 23, no. 1/2, pp. 121–146, 1990.
- [26] S. K. Pal and D. K. D. Majumder, *Fuzzy Mathematical Approach to Pattern Recognition*. New York: Wiley, 1986.
- [27] P. K. Sahoo, S. Soltani, and A. K. C. Wong, "A survey of thresholding techniques," *Comput. Vision, Graphics, Image Processing*, vol. 41, pp. 233–260, 1988.
- [28] J. S. Weszka, "SURVEY: A survey of threshold selection techniques," *Comput. Vision, Graphics, Image Processing*, vol. 7, pp. 259–265, 1978.
- [29] J. N. Kapur, P. K. Sahoo, and A. K. C. Wong, "A new method for grey-level picture thresholding using the entropy of the histogram," *Comput. Vision, Graphics, Image Processing*, vol. 29, pp. 273–285, 1985.
- [30] J. Kittler and J. Illingworth, "Minimum error thresholding," *Pattern Recogn.*, vol. 19, no. 1, pp. 41–47, 1986.
- [31] Q. Z. Ye and P. E. Danielsson, "On minimum error thresholding and its implementations," *Pattern Recogn. Lett.*, vol. 7, pp. 201–206, 1988.
- [32] H. D. Cheng, C. Tong, and Y. J. Lu, "VLSI curve detector," *Pattern Recogn.*, vol. 23, no. 1/2, pp. 35–50, 1990.
- [33] T. W. Ridler and S. Calvard, "Picture thresholding using an iterative selection method," *IEEE Trans. Syst., Man, Cybern.*, vol. PAMI-8, pp. 630–632, Aug. 1978.
- [34] J. Serra, *Image Analysis and Mathematical Morphology*. New York: Academic, 1982.
- [35] J. A. Swets and R. M. Pickette, *Evaluation of Diagnostic Systems—Methods from Signal Detection Theory*. Academic, 1982.
- [36] C. E. Metz, "Some practical issues of experimental design and data analysis in radiological ROC studies," *Investigative Radiol.*, vol. 24, pp. 234–245, 1989.
- [37] H. P. Chan, S. C. B. Lo, L. T. Niklason, D. M. Ikeda, and K. L. Lam, "Image compression in digital mammography: Effects on computerized detection of subtle microcalcifications," *Med. Phys.*, vol. 23, no. 8, pp. 1325–1336, Aug. 1996.
- [38] H. D. Cheng and H. J. Xu, "A novel fuzzy logic approach to contrast enhancement," presented at *14th Int. Conf. Pattern Recognition*, Brisbane, Australia, Aug. 17–20, 1998.